

# Redshift Filtering by *Swift* Apparent X-ray Column Density

Dirk Grupe<sup>1</sup>,

grupe@astro.psu.edu

John A. Nousek<sup>1</sup>, Daniel E. vanden Berk<sup>1</sup>, Peter W.A. Roming<sup>1</sup>, David N. Burrows<sup>1</sup>,  
Olivier Godet<sup>2</sup>, Julian Osborne<sup>2</sup>, Neil Gehrels<sup>3</sup>

## ABSTRACT

We remark on the utility of an observational relation between the absorption column density in excess of the Galactic absorption column density,  $\Delta N_{\text{H}} = N_{\text{H,fit}} - N_{\text{H,gal}}$ , and redshift,  $z$ , determined from all 55 *Swift*-observed long bursts with spectroscopic redshifts as of 2006 December. The absorption column densities,  $N_{\text{H,fit}}$ , are determined from powerlaw fits to the X-ray spectra with the absorption column density left as a free parameter. We find that higher excess absorption column densities with  $\Delta N_{\text{H}} > 2 \times 10^{21} \text{ cm}^{-2}$  are only present in bursts with redshifts  $z < 2$ . Low absorption column densities with  $\Delta N_{\text{H}} < 1 \times 10^{21} \text{ cm}^{-2}$  appear preferentially in high-redshift bursts. Our interpretation is that this relation between redshift and excess column density is an observational effect resulting from the shift of the source rest-frame energy range below 1 keV out of the XRT observable energy range for high redshift bursts. We found a clear anti-correlation between  $\Delta N_{\text{H}}$  and  $z$  that can be used to estimate the range of the maximum redshift of an afterglow. A critical application of our finding is that rapid X-ray observations can be used to optimize the instrumentation used for ground-based optical/NIR follow-up observations. Ground-based spectroscopic redshift measurements of as many bursts as possible are crucial for GRB science.

*Subject headings:* GRBs: general

## 1. Introduction

The *Swift* mission (Gehrels et al. 2004) has revolutionized the study of Gamma-Ray Burst (GRB) afterglows. The mission, which relies upon training sensitive X-ray and optical telescopes on new GRBs as rapidly as possible, has resulted in the accurate positioning of GRB afterglows on a timescale of minutes. Especially for long GRBs, this rapid localization has proven highly effective at identifying afterglows for study at other wavelengths. Already, in about 2 years of operation, *Swift* has localized more than twice as many GRB

afterglows than had been localized in the eight years preceding *Swift* (Burrows & Racusin 2007).

However, *Swift* alone cannot address all the important issues in GRB research. One of the most important GRB parameters is the redshift of a burst. Knowledge of the redshift is not only crucial for determining the luminosity and other physical parameters of the burst, but also permits optimization of ground-based observations. For example a determination of the redshift for high-redshift GRBs requires large telescopes with infra-red sensitivity, because the Lyman absorption edge gets shifted beyond the long wavelength end of the *Swift*-UVOT sensitivity for redshifts above 5 (Roming et al. 2006). GRBs fade rapidly and only spectroscopy can provide reliable redshifts. Therefore, to search for redshifts as high as GRB050904 ( $z=6.29$ ; Kawai et al. 2006), or even to the unexplored  $z \sim 7 - 10$  range, requires

<sup>1</sup> Astronomy Department, Pennsylvania State University, 525 Davey Lab, University Park, PA 16802

<sup>2</sup>Department of Physics & Astronomy, University of Leicester, Leicester, LE1 7RH, UK

<sup>3</sup>Astrophysics Science Division, Astroparticle Physics Laboratory, Code 661, NASA Goddard Space Flight Center, Greenbelt, MD 20771

telescopes in the 8-10 m class making observations within the first night or two of the *Swift* discovery. As listed in this paper, about 6% of all *Swift*-observed GRBs with spectroscopic redshift have redshift  $z > 5$ .

Observing time on such large, world-class telescopes is an extremely precious commodity. Currently the limited number of target of opportunity programs must be triggered based on very limited information in order to spectroscopically observe the many discovered *Swift* GRB afterglow. While nearly all promptly observed *Swift* long GRBs can be localized by the X-ray Telescope (XRT; Burrows et al. 2005), only about 34% are detected by the UV/Optical Telescope (UVOT; Roming et al. 2005a; Roming et al. 2006). Thus observers looking for high redshift bursts can filter the approximately 100 GRBs found by *Swift* each year, by using the criterion: an afterglow is detected by the XRT, but not detected by the UVOT. Unfortunately this criterion alone only reduces the rate of high- $z$  candidates by about 1/3, leaving about 67 GRBs to be observed per year. Moreover, many other factors, e.g. reddening, can result in suppression of afterglow emission in the UVOT sensitivity range (see Roming et al. 2006 for a discussion).

Of course large telescope observers can wait to see if any of the smaller robotic telescopes can select candidates based on the broad-band photometric studies conducted by these telescopes. Often the cost of doing this is to lose several hours waiting for the results of these small telescope studies to be reduced and transmitted, and to be subject to the vagaries of weather and other observing constraints on the ground. Also GRB afterglows decay rapidly. Every hour of waiting reduces the chances of obtaining an optical and/or NIR spectrum of the afterglow and therefore significantly decreases the chances of measuring the redshift of the burst from a spectrum.

To see whether *Swift* XRT data alone can help to provide very early information, we conducted a study of all 55 *Swift* long GRB afterglows with known redshifts by November 2006. On a timescale of one or two hours after the initial XRT detection of a new GRB, the XRT telemeters information to the ground from which many properties of the burst can be determined, including accurate positions, X-ray flux and X-ray spectral

information.

The *Swift* team has been routinely analyzing these data, and reporting them to the world via the GRB Coordinates Network (GCN; Barthelmy et al. 1995). It has been found that the typical afterglow can be fit with a simple power law model spectrum plus the effects of a variable amount of absorbing material (e.g. Stratta et al. 2004; Campana et al. 2006a). This absorbing material can be located either in our Galaxy, in the host galaxy of the GRB, or in intervening gas clouds. As shown on a theoretical basis by Ramirez-Ruiz et al. (2002), extinction in GRBs is expected. Recently Prochaska et al. (2006) presented the results of high-resolution optical spectroscopy of the interstellar medium of GRB host galaxies of *Swift* GRB afterglows. For low redshift bursts, in the observer's rest-frame, the effects of local, and intervening absorption appear at roughly similar energies, and thus the effects are intermixed. For high redshift bursts, the absorbing material in the host galaxy will incur a substantial redshift. The result is that the energy band of the Swift XRT is shifted to higher energies in the GRB rest frame, making it difficult to detect X-ray absorption. Without prior knowledge of the redshift, X-ray observations result in measurements of  $\text{NH}$  that are systematically low compared to the actual absorbing column in the host galaxy.

Thus if we take the apparent absorption column density  $N_{\text{H,fit}}$ , using the photo-electric cross-section as given by Morrison & McCammon (1983), in the observer's rest-frame, and subtract off the known absorption column density in our Galaxy ( $N_{\text{H,gal}}$  as given by Dickey & Lockman 1990), the residual  $\Delta N_{\text{H}} = N_{\text{H,intr}} - N_{\text{H,gal}}$  will reflect the redshifted column density either in the source or in the intervening line-of-sight. If this residual column density appears high, then it is very likely that the GRB is close, because distant GRB absorption effects are overwhelmed by the redshift effect. Of course if the column density is low, we cannot tell whether the GRB is near - with low intrinsic absorption - or far - with either low intrinsic absorption or redshifted high absorption. A similar method has also been proposed to estimate the redshifts of high-redshift quasars (Wang et al. 2004).

We present the values for absorption measured

in the first orbit of data for all 55 Swift GRBs with known spectroscopic redshifts (section 2). The X-ray data are typically available 1-2 hours after the detection of the burst, except for those few bursts for which observing constraints prevent *Swift* from slewing immediately. The relation we are proposing is not a functional prediction (i.e. we do not suggest that GRB redshift is derivable from XRT absorption), but instead we argue that we can predict the maximum redshift of an afterglow on the basis of the excess absorption  $\Delta N_{\text{H}}$ . In section 3 we present the results. Finally, in section 4 we present our conclusion.

Throughout the paper spectral index  $\beta_{\text{X}}$  is defined as  $F_{\nu}(\nu) \propto \nu^{-\beta_{\text{X}}}$ . All errors are  $1\sigma$  unless stated otherwise.

## 2. Observations and data reduction

Table 1 lists all 55 long GRBs with reported spectroscopic redshifts (up to 2006 November) which were observed by *Swift*. We did not include short bursts since they most likely have different physical processes than the long bursts. Furthermore, short burst have typically been detected at relatively low redshifts (e.g. Berger 2006), even though Levan et al. (2006) suggested that the short GRB 060121 is possibly at  $z > 4.5$ . We limit our sample to those bursts with spectroscopic redshifts only, because these are the most reliable redshift measurements. Other methods such as photometric redshifts are less certain because a dropout in bluer filters can also be caused by strong dust reddening.

The XRT data were reduced by the *xrtpipeline* software version 0.10.4 which is part of the HEASOFT version 6.1.1. For XRT Photon Counting mode data (PC; Hill et al. 2004), source photons were selected by *XSELECT* version 2.4 in a circular region with a radius of  $r=47''$  and the background photons were collected in a circular region close by with a radius  $r=137''$ . For bright afterglows with PC mode count rates  $> 1$  count  $\text{s}^{-1}$  the source photons were selected in an annulus that excludes the inner pixels in order to avoid the effects of pileup. For Windowed Timing mode (WT; Hill et al. 2004) data we extracted source and background photons in boxes with a length of 40 pixel each, except from very bright bursts like e.g. GRB 060729 (Grupe et al. 2007)

for which we applied the method as described in Romano et al. (2006). For spectral fitting of the PC and WT mode data only events with grades 0-12 and 0-2, respectively, were included. The X-ray spectra were re-binned by *grppha* 3.0.0 having 20 photons per bin and analyzed by *XSPEC* version 12.3.0 (Arnaud 1996). The auxiliary response files (arf) were created by *xrtmkarf* using arfs version 008. We used the standard response matrix *swxpc0to12\_20010101v008.rmf* for the PC mode data and *swxwt0to2\_20010101v008.rmf* for the WT data. Note: These are standard reduction techniques as used in the first XRT refined analysis GCN circular from *Swift* bursts.

## 3. Results

Table 1 lists the redshift, Galactic absorption column density  $N_{\text{H,gal}}$ ,  $\Delta N_{\text{H}} = N_{\text{H,fit}} - N_{\text{H,gal}}$ , the intrinsic column density  $N_{\text{H,intr}}$  at the redshift of the burst, X-ray energy spectral slope  $\beta_{\text{X}}$ ,  $\chi^2/\nu$  of the power law fit with the absorption column density as a free parameter ( $N_{\text{H,free}}$ ) and fixed to the Galactic value as given by Dickey & Lockman (1990), detection flag for the *Swift* UVOT, and the reference for the spectroscopic redshift measurement. In cases where the free-fit absorption column density  $N_{\text{H,fit}}$  is within the errors consistent with the Galactic value, we set  $\Delta N_{\text{H}}=0$ .

The left panel of Figure 1 compares redshift versus  $\Delta N_{\text{H}}$ . The dotted lines at  $z=2.30$  and  $\Delta N_{\text{H}} = 5.95 \times 10^{20} \text{ cm}^{-2}$  are the medians in  $z$  and  $\Delta N_{\text{H}}$ . These lines are used as cutoff lines to separate between low and high-redshift and low and high excess absorption groups in a  $2 \times 2$  contingency table<sup>1</sup>. The results of grouping these data

<sup>1</sup>We evaluate the statistical significance of our results by use of  $2 \times 2$  contingency tables. A  $2 \times 2$  contingency table is a statistical tool that compares a property of two groups, such as in the present example: low- and high-redshift bursts with or without significant additional absorption above the Galactic column density. The way this method works is the following: assume a number of low redshift bursts  $n = l + k$ , with  $l$  of them having low and  $k$  having high column densities in excess of the Galactic value. The ratio of low to high absorption column objects is then  $l/k$ . For the high-redshift bursts the numbers are  $z = x + y$  with  $x$  representing the number of bursts with low excess absorption column densities and  $y$  representing high excess absorption column densities. If the ratio of low to high absorption bursts in high-redshift bursts is the same as among low-redshift bursts, the number of high-redshift bursts with high absorption column densities is  $y = k \times x/l$ .

by these cutoff lines are given in Table 2. We can immediately see that bursts with high excess absorption column densities  $\Delta N_{\text{H}}$  will most likely be at low redshifts while afterglows with small  $\Delta N_{\text{H}}$  are most likely at high redshifts. From the  $2 \times 2$  contingency table a probability of only  $P=0.0011$  (using a two-tailed Fisher Exact Probability test) that this result is random can be calculated.

Another statistical test to check whether the relation is purely random is the Spearman rank order test. A Spearman rank order test results in a correlation coefficient  $r_s = -0.51$  with a Student's T-test  $T_s = -4.3$  and a probability  $P < 10^{-4}$  of a random distribution.

The right panel of Figure 1 displays the above results as  $\log(1 + z)$  vs.  $\log(1 + \Delta N_{\text{H}})$ . We use this diagram to conservatively draw a line along the envelope of the  $\log(1 + z)$  vs.  $\log(1 + \Delta N_{\text{H}})$  distribution of the bursts, including the errors, in order to determine maximum redshift of a burst with respect to its excess absorption  $\Delta N_{\text{H}}$ . This line is displayed as the dashed line in the right panel of Figure 1 and can be described as:

$$\log(1 + z) < 1.3 - 0.5 \times \log(1 + \Delta N_{\text{H}}) \quad (1)$$

with  $\Delta N_{\text{H}}$  in units of  $10^{20} \text{ cm}^{-2}$ . From this equation we can limit the maximum expected redshift based on the excess absorption. Note that this equation does not estimate the redshift of a burst. The equation only predicts the maximum redshift of a burst. As examples, the redshift of a burst with an excess absorption  $\Delta N_{\text{H}} = 4 \times 10^{21} \text{ cm}^{-2}$  is expected not to exceed  $z=2.1$ ,  $\Delta N_{\text{H}} = 2 \times 10^{21} \text{ cm}^{-2}$  has  $z < 3.4$ , and  $\Delta N_{\text{H}} = 1 \times 10^{21}$  has  $z < 5$ . Also note that the number of bursts with redshifts  $z > 2.3$  (the median redshift) and no excess absorption detected, so the free-fit absorption column density  $N_{\text{H,fit}}$  is consistent with the Galactic value, is three times as high as the number of bursts with no excess absorption and a redshift  $z < 2.3$ . In case we do not detect excess absorption in a burst, most-likely this will be a burst with a redshift  $z > 2.3$ .

Our findings of an observational relation be-

---

The 2x2 contingency table compares the number of objects in each cell to the expected number under this assumption, and can be used to calculate the probability that the deviation from the expected number of objects is just random.

tween the excess absorption column density  $\Delta N_{\text{H}}$  and redshift is due purely to an observational artefact: we only detect any excess absorption in high-redshift bursts which have a very large intrinsic column density, as shown in Figure 2. The dashed line at the lower boundary of the  $N_{\text{H,intr}} - z$  distribution displays the maximum redshift at which an intrinsic column density can be detected in the XRT energy window.

#### 4. Discussion

Our main result is that there is a clear anti-correlation between absorption column density in excess of the Galactic value  $\Delta N_{\text{H}} = N_{\text{H,fit}} - N_{\text{H,gal}}$  and redshift. This relation can be used to limit the range of possible redshifts. GRBs for which early X-ray spectra are consistent with the Galactic absorption column density are most-likely at higher redshifts ( $z > 2$ ), although a few examples of low-redshift GRBs also fall into this category. However, GRBs with a significant excess column density of  $\Delta N_{\text{H}} > 2 \times 10^{21} \text{ cm}^{-2}$  are exclusively at redshifts  $z < 2.0$ .

The strong correlation we find between redshift and intrinsic  $N_{\text{H}}$  is an observational artefact. We can only detect an intrinsic absorber if the absorption column density is large enough to affect the observable energy range. For a  $z=4$  burst the low energy cutoff of the detector at 0.3 keV is at 1.5 keV in the rest frame of the burst. In order to detect any significant additional absorption in the observed energy window above the Galactic value the intrinsic (redshifted) absorption has to be in the order of at least  $10^{22} \text{ cm}^{-2}$ , as shown in Figure 2.

There are a few points one should be cautious about: 1) Our study is biased towards afterglows which have spectroscopic redshifts and are therefore detectable at optical and/or NIR wavelengths. As a result, we 2) may miss afterglows in galaxies seen edge-on. These afterglows would suffer from significant absorption columns on the order of several times  $10^{23} \text{ cm}^{-2}$  as is commonly observed in e.g. Seyfert 2 galaxies. 3) Some of the early XRT WT mode data are not well-fitted by a single absorbed power law model, e.g. GRBs 060614 and 060729 (Mangano et al. 2007; Grupe et al. 2007, respectively). These GRBs display dramatic changes in their X-ray spectra within min-

utes and the spectrum cannot be modelled by one single power law. In some cases the spectra require multi-component spectral models as it is the case for GRB 060729 (Grupe et al. 2007).

The immediate application of our column density - redshift relation is to optimize ground-based optical and NIR follow up observations. We plan to include the redshift limit information in future XRT refined analysis GCNs. Photometric redshifts can also be calculated on the basis of UVOT data (Vanden Berk et al., in preparation). We tested our X-ray method with bursts that have UVOT photometric redshifts, but no spectroscopic redshifts and found that the results agree with each other. The advantage, however, of using the *Swift*-XRT data instead of the UVOT data to estimate a maximum redshift is that *Swift*-XRT data are typically processed faster at the NASA *Swift* Data Center than the UVOT data. This is due to the larger data volume of the UVOT compared to the XRT data. Therefore a redshift prediction can be given faster on the basis of the XRT data than on the UVOT data. This will give ground-based observers at large telescopes a tool to decide which spectrograph to use - an optical spectrograph for the low-redshift bursts and a NIR spectrograph for the high-redshift bursts and will optimize the use of large ground-based telescopes. Note, however, that the purpose of this paper is not to discourage observers from obtaining spectra of bursts with predicted low redshifts. Each spectroscopic redshift - low or high redshift - is important, because it enables us to determine physical parameters of the burst such as the isotropic energy or the break times in the light curve. Therefore we encourage ground-based observers to continue to obtain spectra of afterglows whenever possible. The larger the number of bursts with spectroscopic redshifts the better our understanding of the physics of GRBs will be.

We would like to thank all observers at ground-based optical telescopes for their effort to obtain redshifts of the *Swift* afterglows. We would also like to thank Sergio Campana for discussion related to the XRT calibration, Cheryl Hurkett for sending us a draft of her paper on GRB 050505, and Abe Falcone for various discussions on the determination of the absorption column densities. In particular we want to thank Eric Feigelson for

various discussions on statistics, and our referee Johan Fynbo for a fast and detailed referee's report that significantly improved the paper. This research has made use of data obtained through the High Energy Astrophysics Science Archive Research Center Online Service, provided by the NASA/Goddard Space Flight Center. At Penn State we acknowledge support from the NASA Swift program through contract NAS5-00136.

## REFERENCES

- Arnaud, K. A., 1996, ASP Conf. Ser. 101: Astronomical Data Analysis Software and Systems V, 101, 17
- Barthelmy, S.D., Butterworth, P., Cline, T., Gehrels, N., Fishman, G.J., Kouveliotou, C., & Meegan, C.A., 1995, Ap&SS, 231, 235
- Berger, E., Kulkarni, S.R., Fox, D.B., et al., 2005a, ApJ, 629, 328
- Berger, E., et al., 2005b, GCN 3368
- Berger, E., Price, P.A., & Fox, D.B., 2006a, GCN 4622
- Berger, E., Kulkarni, S.R., Rau, A., & Fox, D.B., 2006b, GCN 4815
- Berger, E., et al., 2006, ApJ, submitted, astro-ph/0611128
- Berger, E., & Gladders, M., 2006, GCN 5170
- Berger, E., 2006, GCN 5962
- Bloom, J.S., Perley, D., Foley, R., Prochaska, J.X., Chen, H.W., & Starr, D., 2005, GCN 3758
- Bloom, J.S., Foley, R.J., Kocevski, D., & Perley, D., 2006a, GCN 5217
- Bloom, J.S., Perley, D., & Chen, H.W., 2006b, GCN 5826
- Burrows, D.N., & Racusin, J.L., 2007, proceedings of the meeting on GRBs, Venice June 2006, in press, astro-ph/0702633
- Burrows, D.N., et al., 2005, Space Science Reviews, 120, 165
- Campana, S., et al., 2006a, A&A, 449, 61

- Campana, S., et al., 2006b, *Nature*, 442, 1008
- Castro-Tirado, A.J., Amado, P., Negueruela, I., Gorosabel, J., Jelínek, M., & A. de Ugarte Postigo, 2006, *GCN* 5218
- Cenko, S.B., et al., 2005, *GCN* 3542
- Cenko, S.B., Berger, E., Djorgovski, S.G., Mahabal, A.A., & Fox, D.B., 2006, *GCN* 5155
- Chen, H.-W., et al., 2005, *GCN* 3706
- Cucchiara, A., Fox, D.B., & Berger, E., 2006a, *GCN* 4729
- Cucchiara, A., Price, P.A., Fox, D.B., Cenko, S.B., & Schmidt, B.P., 2006b, *GCN* 5052
- Dickey, J.M., & Lockman, F.J., 1990, *ARA&A*, 28, 215
- D'Elia, V., et al., 2006a, *GCN* 4520
- D'Elia, V., et al., 2006b, *GCN* 5637
- Dupree, A.K., Falco, E., Prochaska, J.X., Chen, H.-W., & Bloom, J.S., 2006, *GCN* 4969
- Ellison, S.L., et al., 2006, *MNRAS*, 372, L38
- Ferrero, P., et al., 2006, *GCN* 5489
- Foley, R.J., et al., 2005, *GCN* 3483
- Fugazza, D., et al., 2005, *GCN* 3948
- Fugazza, D., et al., 2006, *GCN* 5513
- Fynbo, J.P.U., et al., 2005a, *GCN* 3136
- Fynbo, J.P.U., et al., 2005b, *GCN* 3176
- Fynbo, J.P.U., et al., 2005c, *GCN* 3749
- Fynbo, J.P.U., et al., 2006a, *A&A*, 451, L47
- Fynbo, J.P.U., et al., 2006b, *GCN* 5651
- Fynbo, J.P.U., Malesani, D., Thoene, C.C., Vreeswijk, P.M., Hjorth, J., & Henriksen, C., 2006b, *GCN* 5809
- Gal-Yam, A., et al., 2005, *GCN* 4156
- Gehrels, N., et al., 2004, *ApJ*, 611, 1005
- Grupe, D., et al., 2006, *ApJ*, 645, 464
- Grupe, D., et al., 2007, *ApJ*, submitted, [astro-ph/0611240](http://astro-ph/0611240)
- Halpern, J.P., & Mirabal, N., 2006, *GCN* 5982
- Hill, J.E., et al., 2004, *SPIE*, 5165, 217
- Hill, G., Prochaska, J.X., Fox, D., Schaefer, B., Reed, M., 2005, *GCN* 4255
- Jakobsson, P., et al., 2006a, *A&A*, 447, 897
- Jakobsson, P., et al., 2006b, *A&A*, 460, L13
- Jakobsson, P., et al., 2006c, *GCN* 5782
- Kawai, N., et al., 2006, *Nature*, 440, 184
- Ledoux, C., Vreeswijk, P., Smette, A., Jaunsen, A., & Kaufer, A., 2006, *GCN* 5237
- Levan, A.J., et al., *ApJ*, 648, L9
- Mangano, V., et al., 2007, *A&A*, submitted
- Mirabal, N., & Halpern, J.P., 2006a, *GCN* 4591
- Mirabal, N., & Halpern, J.P., 2006b, *GCN* 4792
- Morrison, R., & McCammon, D., 1983, *ApJ*, 270, 119
- Nardini, M., Ghisellini, G., Ghirlanda, G., Tavecchio, F., Firmani, C., & Lazzati, D., 2006, *A&A*, 451, 821
- Osip, D., Chen, H.-W., & Prochaska, J.X., 2006, *GCN* 5715
- Page, K.L., et al., 2007, *ApJ*, submitted
- Perley, D., Foley, R.J., Bloom, J.S., & Butler, N., 2005, *GCN* 5387
- Price, P.A., 2006, *GCN* 5104
- Price, P.A., Berger, E., & Fox, D.B., 2006, *GCN* 5274
- Piranomonte, S., et al., 2005, *GCN* 4032
- Piranomonte, S., Covino, S., Malesani, D., Fiore, F., Tagliaferri, G., Chincarini, & Stella, L., 2006, *GCN* 5626
- Prochaska, J.X., et al., 2005, *GCN* 3833
- Prochaska, J.X., et al., 2006, *ApJS*, accepted, [astro-ph/0611092](http://astro-ph/0611092)

Quimby, R., Fox, D., Höflich, P., Roman, B.,  
Wheeler, J.C., 2005, GCN 4221

Ramirez-Ruiz, E., Trentham, N., & Blain, A.W.,  
2002, MNRAS, 329, 465

Rol, E., Jakobsson, P., Tanvir, N., Levan, A.,  
2006, GCN 5555

Romano, P. et al. 2006, A&A, 456, 917

Roming, P.W.A., et al., 2005a, Space Science Re-  
views, 120, 95

Roming, P.W.A., et al., 2006, ApJ, 652, 1416

Savaglio, S., Palazzi, E., Ferrero, P., & Klose, S.,  
2007, GCN 6166

Schady, P., et al., 2007, MNRAS, submitted,  
astro-ph/0611081

Soderberg, A.M. Berger, E., & Ofek, E., 2005,  
GCN 4186

Still, M., et al., 2006, GCN 5226

Stratta, G., Fiore, F., Antonelli, L.A., Piro, L., &  
De Pasquale, M., 2004, ApJ, 608, 846

Thoene, C.C., et al., 2006a, GCN 5373

Thoene, C.C., Fynbo, J.P.U., Jakobsson, P.,  
Vreeswijk, P.M., & Hjorth, J., 2006b, GCN  
5812

Wang, J.X., Malhotra, S., Rhoads, J.E., & Nor-  
man, C.A., 2004, ApJ, 612, L109

Watson, D., et al., ApJ, 652, 1011

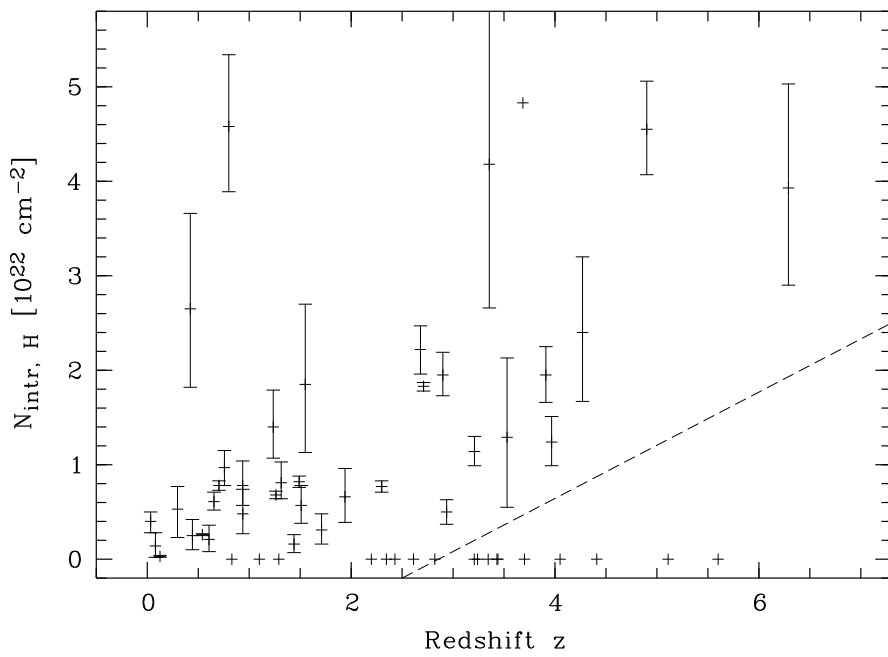


Fig. 2.— Redshift  $z$  vs. the intrinsic column density  $N_{\text{H,intr}}$ . The dashed line marks the redshift limit at which an intrinsic column density can be detected in the XRT.

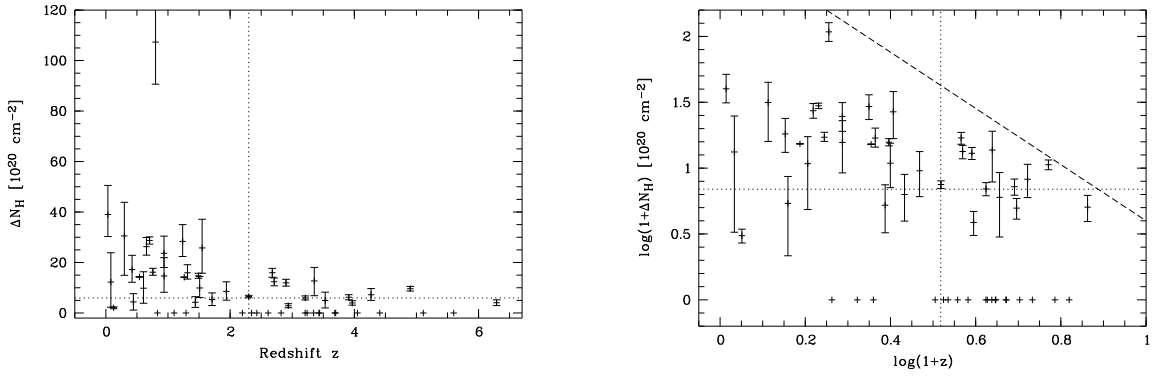


Fig. 1.— Redshift  $z$  vs.  $\Delta N_{\text{H}}$  relation among the *Swift*-observed bursts with spectroscopic redshifts. The left panel displays the direct values while the right panel shows the values with  $\log(1+z)$  and  $\log(1+\Delta N_{\text{H}})$ . The dotted lines display the median values for  $\Delta N_{\text{H}} = 5.00 \times 10^{20} \text{ cm}^{-2}$  and  $z=2.30$  used for the  $2\times 2$  contingency test (see text). The dashed line in the right panel displays the line of the maximum expected value for the redshift as given from equation 1.

TABLE 1

LIST OF ALL LONG BURST GRB AFTERGLOWS WITH *Swift* OBSERVATIONS AND REPORTED REDSHIFTS

GRB	z	$N_{\text{H,gal}}^2$	$\Delta N_{\text{H}}^3$	$N_{\text{H,intr}}^4$	$\beta_{\text{X}}^5$	$\chi^2/\nu$	$N_{\text{H-free}}^6$	$\chi^2/\nu$	$N_{\text{H-fix}}^7$	UVOT <sup>8</sup>	Redshift reference
050126	1.29	5.28	—	—	1.01 $\pm$ 0.18	—	—	16/15	n	Berger et al. (2005a)	
050315	1.94	4.34	8.55 $\pm$ 3.80	0.66 $\pm$ 0.30	1.42 $\pm$ 0.18	43/45	61/46	n	Berger et al. (2005a)		
050318	1.44	2.79	4.23 $\pm$ 2.24	0.16 $\pm$ 0.10	1.03 $\pm$ 0.11	73/74	86/75	y	Berger et al. (2005a)		
050319	3.24	1.13	—	—	1.10 $\pm$ 0.17	27/36	31/37	y	Jakobsson et al. (2006b) <sup>9</sup>		
050401	2.90	4.84	11.96 $\pm$ 1.39	1.95 $\pm$ 0.22	1.05 $\pm$ 0.06	296/258	614/259	n	Watson et al. (2006) <sup>10</sup>		
050408	1.2357	1.74	28.36 $\pm$ 6.60	1.40 $\pm$ 0.39	1.31 $\pm$ 0.20	39/36	120/37	y	Berger et al. (2005a)		
050416A	0.6535	2.07	26.28 $\pm$ 3.37	0.61 $\pm$ 0.09	1.20 $\pm$ 0.12	65/84	320/85	y	Jakobsson et al. (2006a) <sup>11</sup>		
050505	4.27	2.04	7.23 $\pm$ 3.45	2.40 $\pm$ 0.80	1.18 $\pm$ 0.12	51/77	85/78	n	Jakobsson et al. (2006a) <sup>12</sup>		
050525	0.606	9.10	9.81 $\pm$ 5.96	0.21 $\pm$ 0.13	1.05 $\pm$ 0.23	23/27	31/28	y	Jakobsson et al. (2006a) <sup>13</sup>		
050603	2.821	1.19	—	—	0.75 $\pm$ 0.10	30/34	31/35	y	Jakobsson et al. (2006a) <sup>14</sup>		
050730	3.967	3.06	3.97 $\pm$ 0.91	1.24 $\pm$ 0.25	0.71 $\pm$ 0.04	177/174	243/175	y	Jakobsson et al. (2006a) <sup>15</sup>		
050802	1.71	1.78	5.31 $\pm$ 2.66	0.31 $\pm$ 0.17	1.00 $\pm$ 0.12	61/67	77/68	y	Jakobsson et al. (2006a) <sup>16</sup>		
050803	0.422	5.63	17.19 $\pm$ 5.65	2.65 $\pm$ 1.01	1.05 $\pm$ 0.19	57/59	99/60	n	Bloom et al. (2005)		
050820	2.612	4.71	—	—	0.00 $\pm$ 0.04	87/100	87/101	y	Jakobsson et al. (2006a) <sup>17</sup>		
050824	0.83	3.62	—	—	0.83 $\pm$ 0.24	23/20	22/21	y	Jakobsson et al. (2006a) <sup>18</sup>		
050826	0.297	21.70	30.54 $\pm$ 15.6	0.53 $\pm$ 0.30	0.95 $\pm$ 0.26	29/25	45/26	n	Halpern & Mirabal (2006)		
050904	6.29	4.93	4.05 $\pm$ 1.16	3.93 $\pm$ 1.10	0.47 $\pm$ 0.04	126/87	104/92	n	Kawai et al. (2006)		
050908	3.344	2.14	—	—	2.01 $\pm$ 0.41	15/17	15/18	y	Jakobsson et al. (2006a) <sup>19</sup>		
050922C	2.198	3.43	—	—	0.99 $\pm$ 0.11	22/25	22/26	y	Piranomonte et al. (2005) <sup>20</sup>		
051016B	0.9364	3.64	23.67 $\pm$ 6.77	0.78 $\pm$ 0.26	1.13 $\pm$ 0.21	30/32	93/33	y	Nardini et al. (2006) <sup>21</sup>		
051022	0.80	4.06	107.3 $\pm$ 16.7	4.58 $\pm$ 0.76	1.38 $\pm$ 0.22	35/47	206/48	n	Gal-Yam et al. (2005)		
051109A	2.346	17.5	—	—	1.03 $\pm$ 0.11	43/34	43/35	y	Nardini et al. (2006) <sup>22</sup>		
051109B	0.080	13.1	12.26 $\pm$ 11.6	0.14 $\pm$ 0.14	1.16 $\pm$ 0.33	11/15	15/16	n	Perley et al. (2005)		
051111	1.55	5.02	25.77 $\pm$ 11.36	1.85 $\pm$ 0.22	1.77 $\pm$ 0.47	16/12	36/13	y	Nardini et al. (2006) <sup>23</sup>		
060115	3.53	12.60	5.00 $\pm$ 3.00	1.29 $\pm$ 0.84	0.92 $\pm$ 0.12	78/85	86/86	n	D'Elia et al. (2006a)		
060123	1.099	1.48	—	—	0.77 $\pm$ 0.26	11/15	14/16	n	Berger et al. (2006a)		
060124	2.30	9.16	6.51 $\pm$ 0.50	0.77 $\pm$ 0.06	0.36 $\pm$ 0.01	654/453	1215/454	y	Mirabal & Halpern (2006a)		
060206	4.05	0.94	—	—	1.25 $\pm$ 0.34	9/11	13/12	y	Fynbo et al. (2006a)		
060210	3.91	8.52	6.23 $\pm$ 1.03	1.95 $\pm$ 0.29	1.05 $\pm$ 0.04	195/107	315/108	n	Cucchiara et al. (2006a)		
060218 <sup>24</sup>	0.033	11.00	39.01 $\pm$ 11.38	0.40 $\pm$ 0.12	3.13 $\pm$ 0.53	17/26	90/27	y	Mirabal & Halpern (2006b)		
060223A	4.41	5.93	—	—	0.84 $\pm$ 0.15	15/14	16/15	n	Berger et al. (2006b)		
060418	1.49	9.27	14.27 $\pm$ 1.00	0.82 $\pm$ 0.06	1.22 $\pm$ 0.04	218/174	1073/149	y	Ellison et al. (2006) <sup>25</sup>		
060502A	1.51	2.97	9.90 $\pm$ 4.56	0.57 $\pm$ 0.21	2.36 $\pm$ 0.46	64/35	89/36	y	Cucchiara et al. (2006b)		
060510B	4.90	3.78	9.61 $\pm$ 2.22	4.55 $\pm$ 0.51	0.38 $\pm$ 0.03	194/183	238/183	n	Price (2006)		
060512	0.4428	1.43	4.40 $\pm$ 3.24	0.25 $\pm$ 0.17	3.07 $\pm$ 0.38	22/10	23/11	y	Bloom et al. (2006a)		
060522	5.11	4.83	—	—	0.70 $\pm$ 0.19	17/17	17/18	y	Cenko et al. (2006)		
060526	3.21	5.46	5.95 $\pm$ 0.81	1.14 $\pm$ 0.16	0.79 $\pm$ 0.03	217/158	408/159	y	Berger & Gladders (2006) <sup>20</sup>		
060604	2.68	4.55	15.96 $\pm$ 1.72	2.25 $\pm$ 0.25	1.39 $\pm$ 0.07	83/51	392/52	y	Castro-Tirado et al. (2006)		
060605	3.711 <sup>26</sup>	5.11	—	—	1.03 $\pm$ 0.09	31/35	31/36	y	Still et al. (2006) <sup>27</sup>		
060607	2.937	2.67	2.87 $\pm$ 0.82	0.50 $\pm$ 0.13	0.79 $\pm$ 0.04	200/188	240/189	y	Ledoux et al. (2006)		
060614	0.125	3.07	2.07 $\pm$ 0.37	0.03 $\pm$ 0.01	0.45 $\pm$ 0.15	446/256	541/257	y	Mangano et al. (2007) <sup>28</sup>		
060707	3.43	1.76	—	—	0.94 $\pm$ 0.12	13/18	13/9	y	Jakobsson et al. (2006b)		
060714	2.71	6.72	12.36 $\pm$ 1.59	1.83 $\pm$ 0.05	0.98 $\pm$ 0.06	261/252	501/253	y	Jakobsson et al. (2006b)		
060729	0.54	4.82	14.29 $\pm$ 0.09	0.26 $\pm$ 0.01	1.76 $\pm$ 0.04	505/297	1817/298	y	Grupe et al. (2007) <sup>29</sup>		
060904B	0.703	12.10	28.80 $\pm$ 1.45	0.78 $\pm$ 0.05	1.16 $\pm$ 0.04	540/425	2570/426	y	Fugazza et al. (2006)		
060906	3.685	9.66	—	—	1.51 $\pm$ 0.62	12/10	16/11	n	Jakobsson et al. (2006b)		
060908	2.43	2.73	—	—	1.30 $\pm$ 0.28	29/25	31/26	y	Rol et al. (2006)		
060912	0.937	4.23	14.67 $\pm$ 7.25	0.48 $\pm$ 0.26	1.17 $\pm$ 0.25	11/20	27/21	y	Jakobsson et al. (2006b)		
060926	3.208	7.30	—	—	0.97 $\pm$ 0.33	11/15	16/16	y	Piranomonte et al. (2006) <sup>30</sup>		
060927	5.6	5.20	—	—	0.82 $\pm$ 0.30	11/15	11/16	n	Fynbo et al. (2006b)		
061007	1.261	2.22	11.87 $\pm$ 0.04	0.52 $\pm$ 0.02	1.01 $\pm$ 0.01	1072/587	4784/588	y	Schady et al. (2007) <sup>31</sup>		
061100A	0.757	4.87	16.15 $\pm$ 1.20	0.97 $\pm$ 0.19	2.05 $\pm$ 0.11	242/197	579/198	n	Fynbo et al. (2006c)		
061110B	3.44	4.83	—	—	1.04 $\pm$ 0.41	4/3	4/4	n	Thoene et al. (2006b)		
061121	1.314	5.09	15.93 $\pm$ 2.50	0.81 $\pm$ 0.22	0.25 $\pm$ 0.07	290/286	339/287	y	Page et al. (2007) <sup>32</sup>		
061222B	3.355	27.70	12.70 $\pm$ 5.86	4.18 $\pm$ 1.81	1.60 $\pm$ 0.20	78/47	95/47	n	Berger (2006)		

<sup>1</sup>Times after the burst that were selected from the event file<sup>2</sup>Absorption column densities are given in units of  $10^{20}$  cm $^{-2}$ , Galactic  $N_{\text{H}}$  values taken from Dickey & Lockman (1990)<sup>3</sup> $\Delta N_{\text{H}} = N_{\text{H,fit}} - N_{\text{H,gal}}$  in units of  $10^{20}$  cm $^{-2}$ . A dash indicates that the  $N_{\text{H}}$  is consistent with the Galactic value.<sup>4</sup>Column densities of the intrinsic absorber at the redshift of the burst given in units of  $10^{22}$  cm $^{-2}$ .<sup>5</sup>X-ray spectral slopes determined from an absorbed power law fit with the absorption parameter left free, except for those sources where the a free absorption was below the Galactic value. In those cases we fixed the absorption parameter to the Galactic value.<sup>6</sup> $\chi^2/\nu$  of a power law fit with the absorption column density as a free parameter<sup>7</sup> $\chi^2/\nu$  of a power law fit with the absorption column density fixed to the Galactic value<sup>8</sup>UVOT detection in any of the 7 filters including white light with y=detect<sub>10</sub> and n=no detection<sup>9</sup>Redshift originally reported by Fynbo et al. (2005a).<sup>10</sup>Redshift originally reported by Fynbo et al. (2005b).<sup>11</sup>Redshift originally reported by Cenko et al. (2005).<sup>12</sup>Redshift originally reported by Berger et al. (2005a).<sup>13</sup>Redshift originally reported by Foley et al. (2005).

<sup>18</sup>Redshift originally reported by Fynbo et al. (2005b).

<sup>19</sup>Redshift originally reported by Fugazza et al. (2005).

<sup>20</sup>See also Jakobsson et al. (2006b)

<sup>21</sup>Redshift originally reported by Soderberg et al. (2005).

<sup>22</sup>Redshift originally reported by Quimby et al. (2005).

<sup>23</sup>Redshift originally reported by Hill G. et al. (2005).

<sup>24</sup>GRB 060218/SN 2006aj has a very unusual initial spectrum that can not be fitted by a single power law. It requires a strong thermal component (Campana et al. 2006b). Therefore we only used the pc mode data for this unusual burst.

<sup>25</sup>Redshift originally reported by Dupree et al., (2006).

<sup>26</sup>This redshift was revised by Savaglio, S., et al. (2007) to  $z=3.78$ .

<sup>27</sup>See also Ferrero et al. (2006).

<sup>28</sup>Redshift originally reported by Price et al. (2006).

<sup>29</sup>Redshift originally reported by Thoene et al. (2006a).

<sup>30</sup>Improved redshift given by D'Elia et al. (2006b)

<sup>31</sup>Redshift originally reported by Osip et al. (2006) but also see Jakobsson et al. (2006c).

<sup>32</sup>Redshift originally reported by Bloom et al. (2006b).

TABLE 2

2×2 CONTINGENCY TABLE RESULTS FOR THE CUTS AT A REDSHIFT  $z=2.30$  AND  $\Delta N_H = 5.95 \times 10^{20} \text{ cm}^{-2}$ .

	$z \leq 2.30$	$z > 2.30$
$\Delta N_H \geq 5.95 \times 10^{21} \text{ cm}^{-2}$	20	7
$\Delta N_H < 5.95 \times 10^{21} \text{ cm}^{-2}$	8	20